Materials Research Proceedings 41 (2024) 2710-2719 https://doi.org/10.21741/9781644903131-297

Multi-material topology optimization of additively manufactured thermoplastic molds for heat transfer enhancement

STORTI Bruno A.[1,a*], SOBOTKA Vincent[1,b], ÁLVAREZ HOSTOS Juan C.[2,c], LEFEVRE Nicolás[1,d], LE CORRE Steven[1,e], FACHINOTTI Victor[2,f]

[1]Nantes Université, CNRS, Laboratoire de Thermique et Énergie de Nantes, LTeN, UMR 6607, Rue Christian Pauc, Nantes, 44300, Pays de la Loire, France

[2]Centro de Investigación de Métodos Computacionales (CIMEC), Universidad Nacional del Litoral (UNL)/Consejo Nacional de Investigaciones Científicas y Técnicas (CONICET), Colectora Ruta Nac. N° 168 Km 0, Santa Fe, 3000, Argentina

[a]bruno.storti@univ-nantes.fr, [b]vincent.sobotka@univ-nantes.fr, [c]jchostos@cimec.unl.edu.ar, [d]nicolas.lefevre@univ-nantes.fr, [e]steven.lecorre@univ-nantes.fr, [f]vfachinotti@santafe-conicet.gov.ar

Keywords: Injection Molding, Topology Optimization, Metadevices, Additive Manufacturing, FEM

Abstract. For low-volume scale manufacturing of plastic parts, thermoplastic molds made of polymers and printed by additive manufacturing (AM) technology have proved to be a viable alternative to replace expensive and time-consuming steel molds. Nevertheless, due to the relatively low thermal conductivity of the polymers employed for their manufacture, not only the cycle times are increased, but also the surface temperature homogeneity is affected during the cooling of the part, potentially impacting its final quality. On the other hand, the latest advances in AM technology allow the 3D printing of parts with two polymers of different thermophysical properties, opening the possibility for heat flux manipulation within the thermoplastic mold. This work is devoted to the numerical implementation of a topology optimization (TO) methodology to enhance the temperature homogeneity of an injected part during the cooling phase. The proposed scheme relies on the usage of the gradient-free particle swarm optimizer (PSO) in conjunction with filtering techniques to obtain a feasible-to-manufacture multi-material thermoplastic mold. The TO strategy is thoroughly validated against gradient-based techniques found in the related literature conceived for heat flux manipulation in the transient regime. The results show outstanding improvements in the temperature homogeneity of the part when strategically placing the low-conductivity polymer in easy-to-cool regions and the high-conductivity polymer in regions that cool down slower. We further report in this work the possibility of achieving standard deviation values like those obtained by a steel counterpart.

Introduction

Injection molding is a widely employed manufacturing process that is mainly based on injecting a melted polymer inside the cavity of a mold, and then quickly cooling it to have the manufactured plastic part [1]. Due to its high strength and thermal conductivity, steel molds are commonly employed for large batches of products. However, their manufacturing cost is high and the time to produce them is large since multiple complex machining processes are needed depending on the part complexity. Furthermore, when non-straight cooling channels (CCs) are needed within the mold, this becomes particularly hard to manufacture with common machining techniques. On the other hand, additive manufacturing (AM) technology emerged as a matured technology capable of manufacturing complex thermoplastic molds, saving costs while reducing the manufacturing time. Particularly in this work, molds for low batches of products are addressed, either for quick product development or prototyping, where steel molds are not suitable.

The main limitation regarding the use of thermoplastic molds comes from the relatively low thermal conductivity of the polymers commonly employed in AM such as in the material extrusion (MEX) process, for instance. It was shown in recent experimental [2] and numerical [3, 4] works that, for a given manufacturing process setup featuring CCs, the cooling time needed to reach the ejection temperature of the part is highly sensitive to the mold's thermal conductivity. Emphasizing the aforementioned, a slight improvement from 0.21 W/(mK) to 0.33 W/(mK) led to a 30 % reduction in the cycle time [3], for instance. Furthermore, the relatively low mold's thermal conductivity leads not only to extended cycle times but also to an increase of through-surface thermal gradients within the plastic part, which can eventually lead to defects of the final product [5]. In light of the aforementioned, common practices in the thermal optimization of metal injection molds, such as the optimization of the geometry and positioning of CCs, as well as the regulation of coolant flow rate and temperature, may assume a subordinate role in comparison to the proper selection of material for polymeric-based molds. Fortunately, as AM technology evolves, material sciences evolve as well by developing high-performance (filled or not) polymers specifically designed to improve their thermal conductivity [6]. Exploiting the sensitivity of the part cooling velocity to the mold material, this work delves into the feasibility of employing two polymers of different thermal conductivity to enhance the heat transfer within a thermoplastic mold.

It is known from the literature that heat flux manipulation within thermal devices can be achieved by optimizing the distribution of two or more materials with different thermophysical properties to accomplish a desired task [7]. Such devices are often referred to as metadevices, i.e., devices whose microstructure topology is artificially conceived to achieve a specific goal. These goals could include shielding [8,9], reversing [7], cloaking [7,9,10,11], or concentrating [10,11] the heat flux in either the stationary and transient heat transfer regime, with potential applications in the design of electronic, thermal characterization, and energy harvesting devices, among others. While commonly employed numerical approaches to perform the topology optimization (TO) task rely on gradient-based implementations, their rate of success in achieving the imposed task can often be linked to the contrast in thermophysical properties between materials, i.e., greater differences (as seen in materials like steel and polymer) enhance the likelihood of achieving optimal convergence.

In this work, a TO strategy is employed to find a suitable material distribution within a thermoplastic mold to improve the temperature homogeneity at the part surface. The TO scheme followed here is based on using the stochastic particle swarm optimization (PSO) method, where the properties of each element of the finite element mesh are defined by the optimizer. Filtering strategies are proposed in order to avoid checkerboard-type solutions, and to obtain a feasible-to-manufacture material distribution from the numerical results. Both the FEM model and the TO proposed here are first validated with previous results reported in the literature [1,8,12].

Problem Statement and Governing Equations

Study Case: Ribbed Plate Part. We start studying the cooling of a T-shape ribbed plate geometry, as observed in Fig. 1a. This shape is of particular interest it presents hard-to-cool regions, such as the near-rib zone, and easy-to-cool ones, such as corners. The injected part is 3.75 mm thick, and the mold is originally conceived on steel featuring internal CCs whose positions were already optimized in [12] (see Fig. 1b). Due to the non-variation of the geometry in the z-axis, the problem can be modeled as two-dimensional symmetric case (see Fig. 1b).

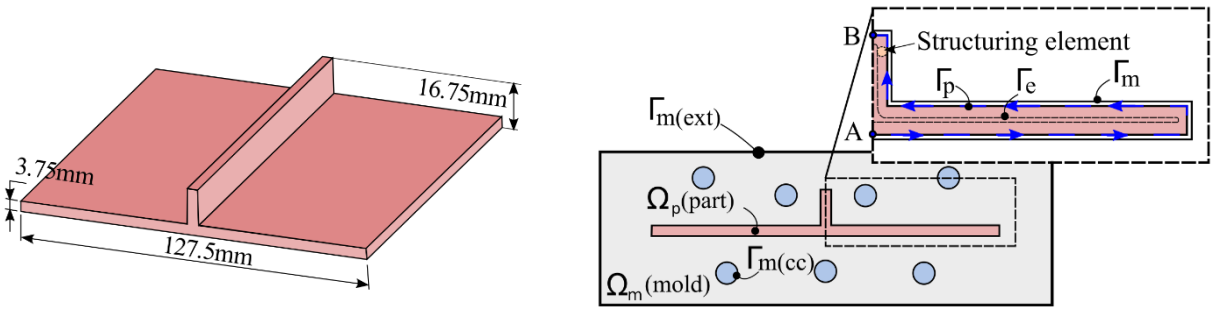

(a) Ribbed plate geometry (b) 2D computational domain

Figure 1: Geometry of a "T" shaped injected part and the mold to produce it considered from [1,12], and to be addressed in this work.

Heat Transfer Governing Equations. The heat released by the melted polymer is transferred by conduction within the mold, and then exchanged through the coolant and the ambient by convection. Therefore, for the numerical heat transfer modeling, the equations to be solved are those of the 2D transient heat conduction problem with convective boundary conditions. The heat equations are to be solved on two domains (see Fig. 1b) accounting for the injected polymer Ω_p, and the insert mold Ω_m. Then, the heat equations yield:

$$\rho_{p,m}\, Cp_{p,m} \frac{\partial T_{p,m}}{\partial t} = \nabla \cdot \left(\lambda_{p,m} \nabla T_{p,m}\right) \quad \forall T_{p,m} \in \Omega_{p,m} \times [0, t_c], \tag{1}$$

where $\rho_{p,m}$, $Cp_{p,m}$ and $\lambda_{p,m}$ stands for the density, heat capacity, and the thermal conductivity of the $\Omega_{p,m}$ domains, $T_{p,m}$ is the unknown temperature, and t_c stands for the cycle time. The injection phase is modeled as an instantaneous non-perfect contact between the molten polymer at a temperature T_{inj} , and the insert at a temperature obtained from the previous cycle. Such an approach is allowed since the duration of the filling stage is negligible with respect to the cooling stage [5,13]. Then, the following initial conditions are employed:

$$T_p(t = 0^+) = T_{inj} \quad \text{in } \Omega_p, \quad \text{and} \quad T_m(t = 0^+) = T_m(t = t_c^-) \text{ in } \Omega_m, \tag{2}$$

where $T_m(t = 0^+) = T_m\ (t = t_c^-\ )$ means that the temperature field T_m of Ω_m at the beginning of a given cycle $t = 0^+$ is considered to be the same as the temperature field at the final time of the previous cycle $t = t_c^-$. The Eq. (2) is subject to the boundary conditions described next. The heat flux at the part-mold interface is modeled as a non-perfect contact condition as follows:

$$-\lambda_p \frac{\partial T_p}{\partial n} = \frac{T_p - T_m}{TCR_{p-m}} \quad \text{at} \quad \Gamma_p \quad \forall t \in [0, t_c]\ , \tag{3}$$

where TCR_{p-m} stands for the thermal contact resistance (TCR) at the part-mold interface Γ_p (see Fig. 1b), and n stands for its outward normal vector. The heat flux exchanged between the mold and the CCs is modeled as:

$$-\lambda_m \frac{\partial T_m}{\partial n} = h_c(T_m - T_c) \ \text{ at } \ \Gamma_{m(cc)} \ \ \forall t \in [0, t_c], \tag{4}$$

where T_c is the coolant temperature, and h_c is the convective coefficient. Finally, the heat transferred from the mold to the environment by convection and radiation is modeled with the following third-type boundary condition:

$$-\lambda_m \frac{\partial T_m}{\partial n} = h_{eq}(T_m - T_{env}), \text{ at } \Gamma_{m(ext)} \ \forall t \in [0, t_c], \quad (5)$$

where $\Gamma_{m(ext)}$ is the boundary of the domain in contact with the surrounding air, T_{env} stands for the ambient temperature, and h_{eq} is an effective exchange coefficient. An additional *erosion surface* Γ_e (see Fig. 1b) internal to Ω_p is considered for analysis, which is basically obtained by rolling internally to Γ_p a circular structuring element of 1.5mm diameter [1].

Thermophysical Properties and Process Parameters. The properties of the injected polymer and the mold material are depicted in Table 1. The mold material originally considered by [12] is steel, and the injected polymer ABS. Two polymers are considered for the thermoplastic mold design: one highly conductive (referred by the super-index c), and one less conductive or *insulating* (referred by the super-index i), envisaging the use of the commercially available PEKK TCPoly ICE 9 and the polycarbonate as potential candidates, respectively. Their thermophysical properties are depicted in Table 1 as well. The parameters of the injection molding process are those reported in [1, 12], and are depicted in Table 2. According to such parameters, a convective coefficient $h_c = 27810$ W/(m^{2}K) is estimated, and $h_{eq} = 10$ W/(m^{2}K) is adopted from [3,4]. Regarding TCR values, 1.10^{-4} m^{2}K/W is employed for polymer-steel contact [1,5], and 1.10^{-2} m^{2}K/W for polymer-polymer contact [3,4].

Table 1: Material properties of the steel and thermoplastic molds, and of the injected polymer.

Steel mold	Injected polymer	Thermoplastic mold	
$\boldsymbol{\lambda_m^s}$=36.5 [W/(mK)]	λ_p=0.25 [W/(mK)]	λ_m^i=0.20 [W/(mK)]	λ_m^c=2.0 [W/(mK)]
$\boldsymbol{\rho_m^s}$=7820 [kg/m^3]	ρ_p=938 [kg/m^3]	ρ_m^i=1210 [kg/m^3]	ρ_m^c=1500 [kg/m^3]
$\boldsymbol{Cp_m^s}$=460 [J/(kgK)]	Cp_p=1800 [J/(kgK)]	Cp_m^i=1300 [J/(kgK)]	Cp_m^c=1300 [J/(kgK)]

Table 2: Injection molding parameters [12].

Fluid temperature	Flow rate	Cycle time	Injection temperature
$\boldsymbol{T_c}$= 303 [K]	$\dot{Q}$= 364 [cm^3/s]	t_c= 23.5 [s]	T_{inj}= 503 [K]

Steel vs. Thermoplastic Mold Thermal Performance. Prior to address the optimization stage, it is of interest to compare the thermal performance of the original steel insert with respect to the highly conductive thermoplastic one. Due to the lower heat diffusivity of the thermoplastic material, t_c needs to be inevitably increased to reach the ejection temperature at the erosion surface. Hence, a parametric study was performed assessing the time needed for the plastic mold case to reach the ejection temperature at Γ_e, and to assess the temperature standard deviation at Γ_p. Then, the outputs to study are the mean temperature of the part ($\overline{T_p}$), mean temperature of the erosion ($\overline{T_e}$), and temperature standard deviation at the part surface (σ_p), all at the ejection time (t_e), and are computed as follows:

$$\overline{T}_p(t_e) = \frac{1}{\Gamma_p}\int_{\Gamma_p} T_p(t_e)d\Gamma, \qquad \sigma_p(t_e) = \left(\frac{1}{\Gamma_p}\int_{\Gamma_p}\left(T_p(t_e) - \overline{T}_p\right)^2 d\Gamma\right)^{1/2}, \quad (6)$$

considering that $\overline{T_e}$ is computed analogously to $\overline{T_p}$ but at Γ_e.

The heat transfer problems were solved with the open-source code PETScFEM (PF) on an unstructured mesh of 13570 triangular elements with a time step of $\Delta t = 0.5$ s for the steel case, and with $\Delta t = 5$ s for the thermoplastic mold scenario. Both the spatial and time discretizations

were derived from a convergence study, resulting in excellent agreement with the results reported in [1] performed in COMSOL (see Fig. 2a and Table 3). The results of the parametric study are presented in Table 3. It can be observed that for $\overline{T_e}$ to reach an ejection temperature below ≈ 335-336 °C (steel case), a $t_c = 140$ s was needed by the thermoplastic mold. Despite of increasing t_c, it can be noticed that the temperature homogeneity at Γ_p is severely affected, increasing σ_p by ≈ 136 %. This can be also observed from Fig. 2a. While the maximum delta temperature $\Delta T = (T_{\Gamma_p}^{max} - T_{\Gamma_p}^{min})$ is of roughly 7 °C for the steel case, such a delta increases to ≈ 23 °C for the thermoplastic case. It can be seen from Fig. 2b that due to the high heat diffusivity of steel, the through-thickness temperature gradients are high, and the through-surface gradients are reduced. In contrast, the opposite scenario is observed for the thermoplastic mold, where low through-thickness and high through-surface temperature gradients are observed. The thermal enhancement and optimization of the thermoplastic mold to improve σ_p while reaching the ejection temperature at Γ_e is the main concern of the next sections.

Table 3: Parametric study performed on the thermoplastic mold for different t_c.

	Steel [1]	Steel (PF)	Thermoplastic (PF)				
$\boldsymbol{t_c}$ [s]	23.5	23.5	125	130	135	140	145
$\overline{\boldsymbol{T_e}}$ [K]	335.6	336.31	340.10	337.97	335.98	334.12	332.38
$\overline{\boldsymbol{T_p}}$[K]	310.7	310.82	336.73	334.96	333.31	331.76	330.31
$\boldsymbol{\sigma_p}$[K]	1.43	1.42	3.81	3.65	3.50	3.37	3.26

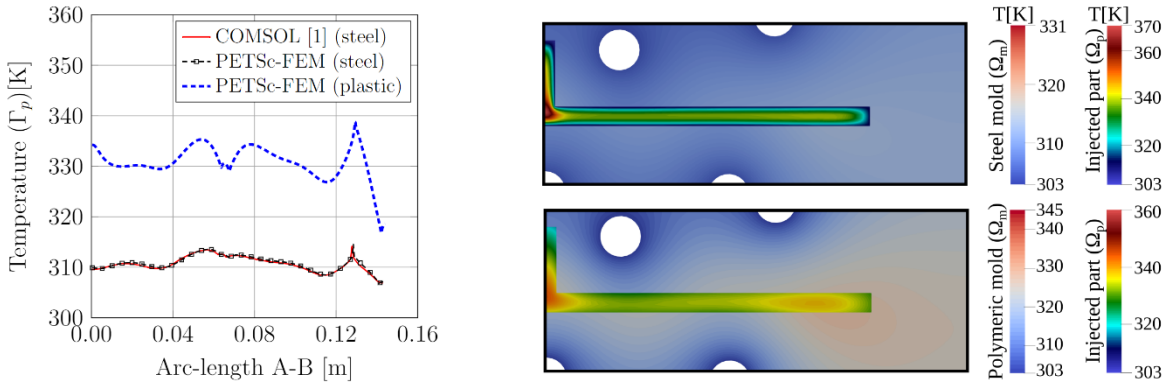

(a) (b)

Figure 2: Temperature fields obtained by the steel and thermoplastic injection molds at 23.5 s and 140 s, respectively, at (a) A-B arc of Γ_p(Fig. 1b), and (b) within the mold and part.

Topology optimization for transient heat flux manipulation

TO-FEM Modeling. Let us consider the semi-discretized FEM form of Eq. (1):

$$\boldsymbol{C\dot{T} + KT = Q}, \tag{7}$$

where **C**, **K** and **Q** are the global capacitance matrix, conduction matrix, and heat load vector, respectively, which are defined as:

$$\boldsymbol{C} = \int_\Omega \boldsymbol{N^T} \rho C_p \boldsymbol{N}\ d\Omega, \qquad \boldsymbol{K} = \int_\Omega \boldsymbol{B^T}\, \lambda \boldsymbol{B}\, d\Omega, \qquad \boldsymbol{Q} = -\int_\Gamma \boldsymbol{N}^T q\, d\Gamma, \tag{8}$$

being $B_{ij} = \partial N_i / \partial x_j$, such that $\nabla T \approx \boldsymbol{BT}$, and the temperature field is approximated as $T(\boldsymbol{x}, t) \approx Nj\ (\boldsymbol{x}) T_j(t) = \boldsymbol{N}(x)\boldsymbol{T}(t)$, where N_j is the shape function associated to the node j of the

discretized finite element space of Ω, and T_j the unknown temperature of the node. For the time discretization we consider a backward Euler scheme throughout this work.

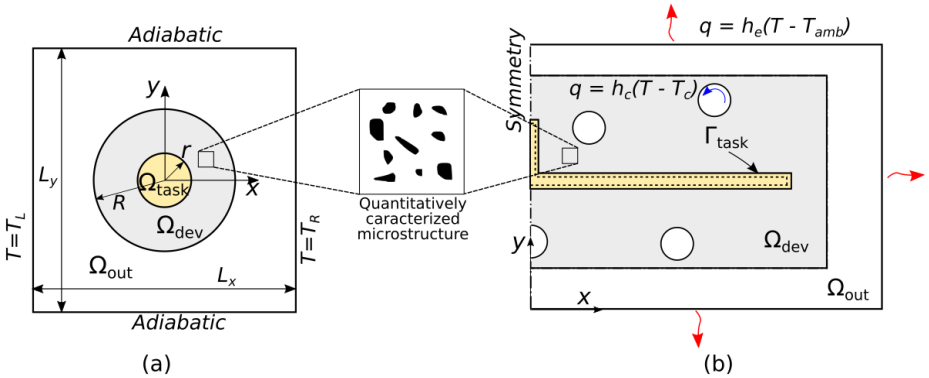

Figure 3: Representative scheme of computational Ω_{dev}: (a) a reference case reported in [8] and used here for validation, and (b) the actual injection mold domain to be optimized in this work.

Now, let us consider a metadevice in a non-homogeneous region $\Omega_{dev} \subset \Omega$ (see Fig. 3) where a design variable vector $\boldsymbol{P}$ of equal size of the finite element mesh of Ω_{dev} will define the type of material on each mesh element. Consequently, $\boldsymbol{C} = \boldsymbol{C}(\boldsymbol{P})$ and $\boldsymbol{K} = \boldsymbol{K}(\boldsymbol{P})$, with $\boldsymbol{P} = [p_1, p_2, \ldots, p_N]$, being N the number of finite elements in Ω_{dev}. Then, inevitably, the transient temperature field in the whole Ω will depend on $\boldsymbol{P}$, i.e., $T = T(x, t, \boldsymbol{P})\ \forall x \in \Omega$. Then, our TO problem summarizes in finding the appropriate set of parameters $\boldsymbol{P}$ in order to accomplish a desired behavior of the heat flux in a given Ω_{task} (Fig. 3a) or Γ_{task}(Fig. 3b). Certainly, our main goal will be to improve temperature homogeneity at $\Gamma_{task} = \Gamma_p$, however, an additional case will be first addressed at Ω_{task} to validate our methodology.

PSO and Filtering Algorithm. The optimization procedure for material distribution in the TO followed here is based on the use of PSO along with density and topological filters, and it is briefly described as follows (please see Fig. 4a): 1) The PSO proposes a vector of parameters $\boldsymbol{P}$ where each element in Ω_{dev} is defined as a continuous value in the [0,1] range; 2) the following density filter [14] is applied aiming to avoid checker-board patterns:

$$p^{(e)} = \frac{\sum_i \langle r^{(e)} - \Delta_{ei} \rangle\, p^{(i)}}{\sum_i \langle r^{(e)} - \Delta_{ei} \rangle}, \tag{9}$$

where $p^{(e)}$ is the design value of a given element e, $r^{(e)}$ is a predefined radius distance from the center of the element, Δ_{ei} is the distance between the i-th and e-th elements, and $p^{(i)}$ stands for the design variable of the i-th element; 3) a threshold is applied to either obtain a conductive/insulating polymer material on each element (threshold value of $w = 0.5$ [14]); 4) single isolated elements that do not share neighbors of the same species are converted into the alternative material; 5) the regions with the same type of material are grouped in sets; 6) those groups who do not accomplish a minimum size ($A \geq 63.6\text{mm}^2$, which is the CC area for reference) are converted in the alternative material. Steps 5) and 6) are performed for the sake of feasible-to-manufacture resulting designs, and two iterations may be needed.

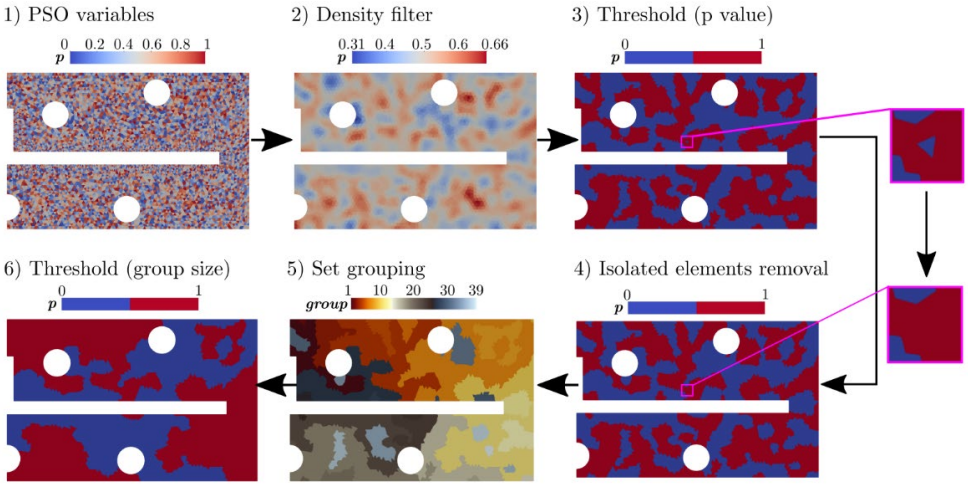

Figure 4: Filtering procedure in the PSO-based TO approach.

Gradient-based and Gradient-free TO Approaches in the Transient Regime. Prior to apply the proposed gradient-free TO scheme to the injection mold design, it is convenient to assess its performance on a transient heat transfer scenario. Hence, the case reported in [8] of Fig. 3a is considered here, where the computational domains start at $T = 293$ K, and the right side temperature is fixed at $T_R = 293$ K. The left side temperature is first increased linearly with time until it reaches $T_L = 333$ K at 520 s and maintained until a first steady regime is reached at 10647 s, and it is subsequently subjected to a further lineal increment to $T_L = 343$ K at t =10825 s, and maintained until finishing the transient heat conduction analysis at $t = t_f$ =19500 s. The main goal is to minimize the function $f_{obj} = (1/\mathrm{t_f}) \int_0^{t_f} g(\boldsymbol{P}, t)dt/f_0$, where f_0 is a constant, and $g(\boldsymbol{P}, t)$ being defined as:

$$g(\boldsymbol{P}, t) = \left[\frac{1}{\Omega_{task}} \int_{\Omega_{task}} \left|\left|q(\boldsymbol{P}, \boldsymbol{x}, t)\right|\right|^2 d\Omega\right]^{1/2}, \tag{10}$$

which represents the total heat flux in Ω_{task}. Ω_{out} is made of Gad Pad material, Ω_{task} is made of PMMA polymer, and Ω_{dev} can be either conformed by PMMA or copper. A symmetry case was considered where the upper half of Ω was meshed by 200x100 structured quadrangular elements, where 3614 finite elements (hence, variables) defined Ω_{dev}. We refer the reader to [8] for detailed information of the materials properties and the numerical setup.

After 13500 f_{obj} evaluations and roughly 8hs solving in parallel on 80 cores, the solution was converged. The results are presented and compared in Fig. 5. Despite of the dissimilarity in materials distribution obtained by the TO proposed in this work (see Fig. 5b) with respect to that reported in the literature (see Fig. 5a), it can be observed from Fig. 5c that the PSO-based solution successfully accomplished the heat flux shielding task. Furthermore, the PSO-based TO slightly outperformed the gradient-based one in the close-to-stationary state regimes.

TO results on a 3D printed thermoplastic injection mold

Problem Definition. The PSO-based TO is applied to a mold design in this section. The two polymers considered as candidate materials for Ω_{dev} (see Fig. 3b) are those from Table 1. The objective function (f_{obj}) is to minimize $\sigma_p(t_e)$ subject to the constraint $\overline{T_e} < 336$ K. A total of 7733 variables were handled by PSO, corresponding to the number of elements at Ω_{dev}. For each evaluation of f_{obj}, 8 injection cycles were performed using a Δt = 5 s, and each cycle with a total duration of $t_f = 140$ s. The f_{obj} evaluations were solved in parallel in the HPC cluster of Pays de

la Loire (CCIPL), where each simulation took approximately 2 minutes in one single core, and the total optimization process took roughly 12 hours in 40 cores.

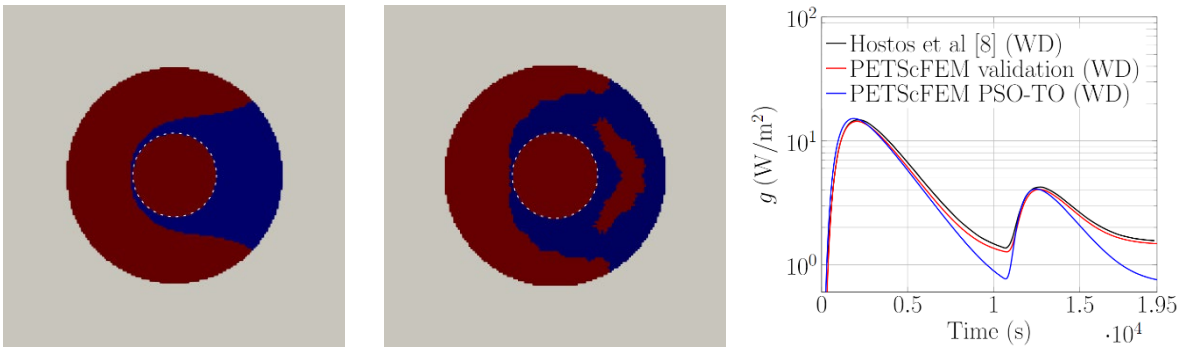

(a) Gradient-based [8] (b) PSO-based TO (c) Comparison.

Figure 5: TO solutions obtained by the gradient-based approach [8], and the gradient-free proposed in this work. In (a) and (b) blue regions represent copper material, while red zones represent PMMA material. In (c) the heat flux in Ω_{task} in time is compared.

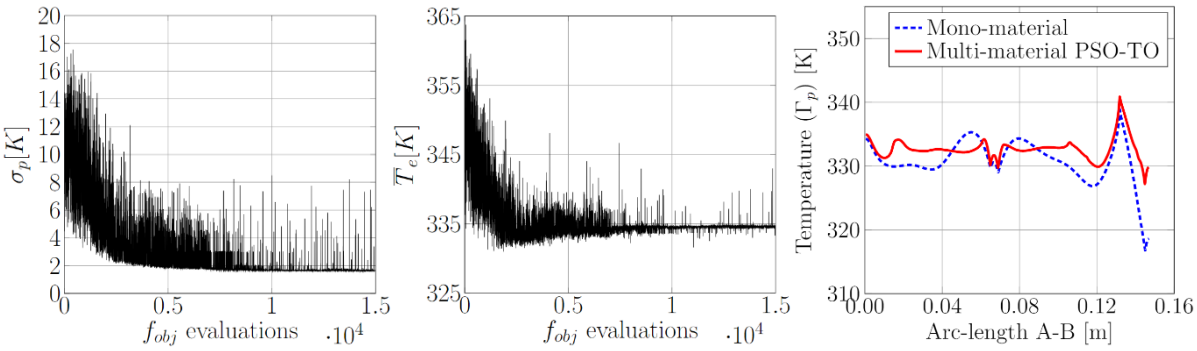

(a) (b) (c)

Figure 6: Results obtained by the topologic optimization scheme: (a) convergence of the objective function, (b) constraint computation, (c) temperature at A-B in Γ_p (see Fig. 1b).

Results Obtained by the PSO-TO in the Injection Mold. The convergence tendency of f_{obj} is evident from Fig. 6a, and the final best value was σ_p = 1.62 K after reaching 15000 f_{obj} evaluations. The accomplishment of the maximum temperature constraint at Γ_e can be observed in Fig. 6b, and the resulting $\overline{T}_e$ was 334.68 °C. The results are summarized in Table 4 where it can be deduced that, for the same cycle time (t_f = 140 s), a marked improvement is obtained in the temperature homogeneity by combining the two thermoplastics, reducing σ_p by 52 %, and obtaining a similar value to that of steel.

Table 4: Results obtained by the mono-material and the optimized multi-material molds.

	Steel	Plastic (mono-material)	Plastic (multi-material)
t_f [s]	23.5	140	140
$\overline{T}_e$ [K]	336.31	334.12	334.68
$\overline{T}_p$ [K]	310.82	331.76	332.67
σ_p [K]	1.42	3.37	1.62
ΔT_{Γ_2} [K]	7,14	23.56	13.32

It can be seen from the profile temperature presented in Fig. 6c that the main peak of delta temperature is given near the central zone of the T-shaped part (arc length = 0.13 m). This region is of course, the most challenging one to evenly cool down. The optimized topology of the multi-material injection mold is presented in Fig. 7. It is interesting to notice that the scheme proposes the insulating polymer mainly at the corners of the T-shaped part. This is explained by the fact that such regions with high surface-to-volume ratios cool down quicker than other regions. On the other hand, the opposite occurs at the near-ribbed region of the piece with a slower cooling, and thus, the scheme proposes the high-conductive polymer at its surroundings. In Fig. 8 are represented the temperature field within the injected part at $t_e = 140$ s for the mono-material and the multi-material optimized molds. The improvement in temperature homogeneity at the end of cooling is very marked for the optimized mold, where, if disregard the central part of the piece, the temperatures remain fairly constant.

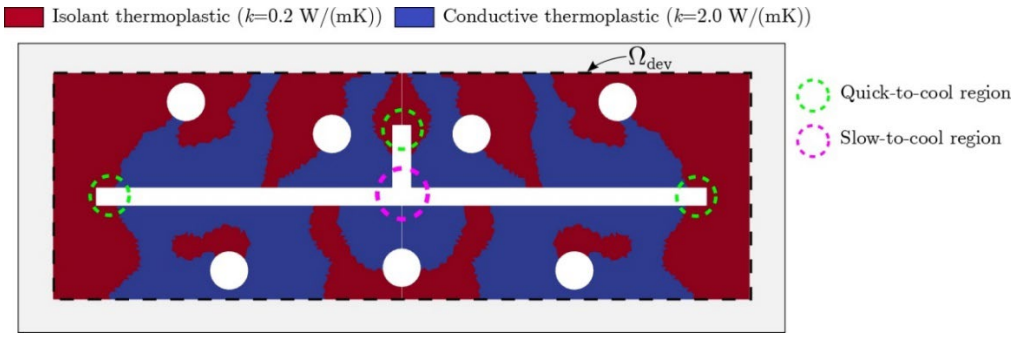

Figure 7: TO result of material distribution within the mold.

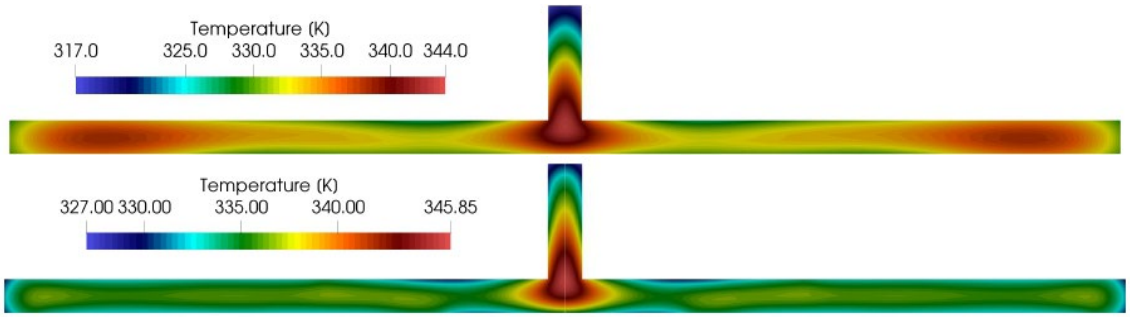

Figure 8: Temperature at the T-shaped injected part at $t_e = 140$ s, obtained by the non-optimized mono-material mold (top), and the optimized multi-material thermoplastic mold (bottom).

Conclusions

A numerical scheme for topology optimization of a thermoplastic injection mold was presented in detail. The scheme proved to successfully handle transient heat flux manipulation addressing complex geometries and complex heat transfer scenarios such as those encountered in the injection molding process featuring thermal contact resistances, cooling channels, and multiple injection cycles. The performance of the scheme was tested on a heat flux shielding scenario in the transient regime and the results were compared with those of the literature. The gradient-free TO scheme proposed here proved to slightly outperform the gradient-based TO approach. The methodology was successfully applied to the thermal design of thermoplastic injection mold combining two polymers of different thermal conductivity. It was shown that by employing the low-conductivity polymer at easy-to-cool regions such as corners, the standard temperature deviation at the part surface can be improved by 52 % while employing the same cycle time of the highly conductive mono-material case. Furthermore, the delta temperature at the part surface can be reduced by up

to 10 °C when employing the multi-material thermoplastic mold. Future works comprise addressing three-dimensional cases featuring complex geometries with the consequent larger number of design variables.

References

[1] A. Agazzi, Contribution à l'optimisation de la thermique des outillages dans le procédé d'injection des polymères thermoplastiques, Ph.D. thesis, Université de Nantes (2011).
[2] C.-C. Kuo, S.-X. Qiu, G.-Y. Lee, J. Zhou, H.-Q. He, Characterizations of polymer injection molding tools with conformal cooling channels fabricated by direct and indirect rapid tooling technologies, Int. J. Adv. Manuf. Technol. 117 (2021) 343–360. https://doi.org/10.1007/s00170-021-07778-w
[3] B. A. Storti, V. Sobotka, Thermal design of cooling channels in an injection plastic mold by overset-based numerical optimization technique, in: International Heat Transfer Conference Digital Library, Begel House Inc., 2023. https://doi.org/10.1615/IHTC17.210-10
[4] B. A. Storti, V. Sobotka, A numerical framework for three-dimensional optimization of cooling channels in thermoplastic printed molds, Appl. Therm. Eng. 238 (2024) 121988. https://doi.org/10.1016/j.applthermaleng.2023.121988
[5] A. Agazzi, V. Sobotka, R. LeGoff, Y. Jarny, Optimal cooling design in injection moulding process – a new approach based on morphological surfaces Appl. Therm. Eng. 52 (1) (2013) 170–178. https://doi.org/10.1016/j.applthermaleng.2012.11.019
[6] A. R. J. Hussain, A. A. Alahyari, S. A. Eastman, C. Thibaud-Erkey, S. Johnston, M. J. Sobkowicz, Review of polymers for heat exchanger applications: Factors concerning thermal conductivity, Appl. Therm. Eng. 113 (2017) 1118–1127. https://doi.org/10.1016/j.applthermaleng.2016.11.041
[7] I. Peralta, V. D. Fachinotti, J. C. Alvarez Hostos, A brief review on thermal metamaterials for cloaking and heat flux manipulation, Adv. Eng. Mater. 22 (2) (2020) 1901034. https://doi.org/10.1002/adem.201901034
[8] J. C. A. Hostos, B. Storti, N. Lefevre, V. Sobotka, S. L. Corre, V. D. Fachinotti, Design via topology optimisation and experimental assessment of thermal metadevices for conductive heat flux shielding in transient regime, Int. J. Heat Mass Transf. 212 (2023) 124238. https://doi.org/10.1016/j.ijheatmasstransfer.2023.124238
[9] G. V. Alekseev, D. A. Tereshko, Particle swarm optimization-based algorithms for solving inverse problems of designing thermal cloaking and shielding devices, Int. J. Heat Mass Transf. 135 (2019) 1269–1277. https://doi.org/10.1016/j.ijheatmasstransfer.2019.02.072
[10] I. Peralta, V. D. Fachinotti, A. A. Ciarbonetti, Optimization-based design of a heat flux concentrator, Sci. Rep. 7 (1) (2017) 40591. https://doi.org/10.1038/srep40591
[11] I. Peralta, V. D. Fachinotti, Optimization-based design of heat flux manipulation devices with emphasis on fabricability, Sci. Rep. 7 (1) (2017) 6261. https://doi.org/10.1038/s41598-017-06565-6
[12] L. Q. Tang, K. Pochiraju, C. Chassapis, S. Manoochehri, A Computer-Aided Optimization Approach for the Design of Injection Mold Cooling Systems, J. Mech. Des. 120 (2) (1998) 165–174. https://doi.org/10.1115/1.2826955
[13] V. Sobotka, A. Agazzi, N. Boyard, D. Delaunay, Parametric model for the analytical determination of the solidification and cooling times of semi-crystalline polymers, Appl. Therm. Eng. 50 (1) (2013) 416–421. https://doi.org/10.1016/j.applthermaleng.2012.07.019
[14] A. E. Albanesi, I. Peralta, F. Bre, B. A. Storti, V. D. Fachinotti, An optimization method based on the evolutionary and topology approaches to reduce the mass of composite wind turbine blades, Struct. Multidiscipl. Optim. 62 (2020) 619–643. https://doi.org/10.1007/s00158-020-02518-2